

Measurement of top quark pair production with the ATLAS detector

Aras Papadelis*[†]

Stockholm University

E-mail: Aras.Papadelis@cern.ch

A measurement of the production cross-section for top quark pairs ($t\bar{t}$) in pp collisions at $\sqrt{s} = 7$ TeV is presented, using data recorded with the ATLAS detector at the Large Hadron Collider. Events are selected for two different topologies: single lepton (electron e or muon μ) with large missing transverse energy and at least four jets, and dilepton (ee , $\mu\mu$ or $e\mu$) with large missing transverse energy and at least two jets. The inclusive top quark pair production cross-section is measured to be

$$\sigma_{t\bar{t}} = 145 \pm 31 \begin{matrix} +42 \\ -27 \end{matrix} \text{ pb}$$

where the first uncertainty is statistical and the second systematic. The measurement agrees with perturbative QCD calculations.

Workshop on Discovery Physics at the LHC -Kruger 2010

December 05-10, 2010

Kruger National Park, Mpumalanga, South Africa

*Speaker.

[†]On behalf of the ATLAS collaboration

1. Introduction

The observation of top quark pair ($t\bar{t}$) production is one of the milestones for the early LHC physics programme; $t\bar{t}$ production is also an important background in various searches for physics beyond the Standard Model (SM) [1], and new physics may give rise to additional $t\bar{t}$ production mechanisms or modification of the top quark decay channels. In the Standard Model the $t\bar{t}$ production cross-section in pp collisions is calculated to be $164.6^{+11.4}_{-15.7}$ pb [2] at a centre of mass energy $\sqrt{s} = 7$ TeV assuming a top mass of 172.5 GeV, and top quarks are predicted to decay to a W -boson and a b -quark ($t \rightarrow Wb$) nearly 100% of the time. Events with a $t\bar{t}$ pair can be classified as ‘single-lepton’, ‘dilepton’, or ‘all hadronic’ by the decays of the two W bosons: a pair of quarks ($W \rightarrow q\bar{q}$) or a lepton-neutrino pair ($W \rightarrow \ell\nu$), where ℓ refers to a lepton. This paper presents a top quark-pair production cross-section measurement at $\sqrt{s} = 7$ TeV using ATLAS [3], a general purpose detector at the Large Hadron Collider at CERN. ATLAS is designed to precisely measure electrons, muons, missing transverse energy and jets. This measurement utilizes data corresponding to an integrated luminosity of 2.9 pb^{-1} . The dominant backgrounds to the $t\bar{t}$ signal are estimated using data-driven techniques.

2. Event and object selection

The reconstruction of $t\bar{t}$ events makes use of electrons, muons and jets, and of missing transverse energy $E_{\text{T}}^{\text{miss}}$ which is a measure of the energy imbalance in the transverse plane and is used as an indicator of undetected neutrinos. Events are triggered by single lepton (electron or muon) triggers that are fully efficient in the range $p_{\text{T}} > 20$ GeV and at least one primary vertex with at least five tracks is required. Electron candidates are based on calorimeter clusters matched to Inner Detector (ID) tracks (see definition in Ref. [4]) and required to fulfill $p_{\text{T}} > 20$ GeV and $|\eta_{\text{cluster}}| < 2.47$. Clusters in the transition region between the barrel and the endcap calorimeters ($1.37 < |\eta| < 1.52$) are excluded. Criteria on shower shape and hadronic leakage are imposed to reject hadronic background. Photon conversions are suppressed by a pixel detector hit requirement. Muon candidates are identified by combined tracking using the ID and Muon Spectrometer (MS). Tracks are required to have $p_{\text{T}} > 20$ GeV and be within $|\eta| < 2.5$. Background due to leptons from decays of hadrons produced in jets are suppressed by isolation requirements in the calorimeter and the tracker, as detailed in Ref. [5]. Jets are reconstructed with the anti- k_r algorithm [6] ($R = 0.4$) from topological clusters in the calorimeter. Jets within close proximity to an electron candidate are removed to avoid double-counting of electrons as jets. Jets from b -quarks are selected by the existence of a secondary vertex spatially displaced from the primary vertex. The missing transverse energy is constructed from a vector sum of all calorimeter cells contained in topological clusters. Cells are calibrated to the electron or hadronic energy scale depending on if the cells belong to an electron candidate or a jet respectively. Acceptances and efficiencies are extracted from Monte Carlo simulations and verified with data in control regions which are depleted of $t\bar{t}$ events. Scale factors for lepton efficiencies are derived from a comparison between data and simulation in the Z -boson mass window.

3. Single lepton channel

The single lepton $t\bar{t}$ final state is characterized by an isolated lepton with relatively high p_T and missing transverse energy corresponding to the neutrino from the W leptonic decay, two b -quark jets and two light jets from the hadronic W decay. Events are selected that contain exactly one reconstructed lepton and fulfill $E_T^{\text{miss}} > 20$ GeV and $E_T^{\text{miss}} + m_T(W) > 60$ GeV¹. These requirements efficiently suppress background from QCD multi-jets. At least 4 jets with $p_T > 25$ GeV and $|\eta| < 2.5$ are required and at least one of the jets has to be b -tagged. The dominant background contributions come from W +jets and QCD multi-jets, where the latter mainly enters the analysis through a jet misreconstructed as a lepton or through a semileptonic b -quark or c -quark decay. Their contributions are difficult to model precisely with simulation and are therefore estimated using a set of data-driven approaches further detailed in [5]. The smaller sources of background, single top and Z +jets are estimated from simulation. The estimated product of acceptance and branching fraction for $t\bar{t}$ events, measured from Monte Carlo samples, are $(3.1 \pm 0.7)\%$ and $(3.2 \pm 0.7)\%$ for e +jets and μ +jets respectively. Table 1 summarizes the observed event yield, the estimated total background and the $t\bar{t}$ signal. A number of sources of systematic uncertainty are accounted for. The dominant contributions are: luminosity measurement, initial state and final state radiation, b -tagging, jet energy reconstruction and background rate normalisation. Figure 1 shows

	e +jets	μ +jets	combined
Observed	17	20	37
Total est. background	7.5 ± 3.1	4.7 ± 1.7	12.2 ± 3.9
$t\bar{t}$	$9.5 \pm 4.1 \pm 3.1$	$15.3 \pm 4.4 \pm 1.7$	$24.8 \pm 6.1 \pm 3.9$

Table 1: Observed event yield, estimated total background and $t\bar{t}$ signal, for electrons and muons separately and combined. The uncertainty on the total background includes statistical uncertainties in control regions and systematic uncertainties. The first quoted uncertainty on the $t\bar{t}$ signal yield is statistical, while the second is from the systematics on the background estimation.

the observed jet multiplicity together with the sum of all expected contributions. The largest fraction of $t\bar{t}$ events is concentrated in ≥ 4 -jets bin, which is defined as the signal region and used for the $t\bar{t}$ signal extraction. Other regions are used as control samples for the determination of backgrounds. As a cross-check that the selected events are from $t\bar{t}$ decays, the invariant mass is formed from the combination of the three jets (with $p_T > 20$ GeV) with the highest vector sum p_T . This combination is expected to reconstruct [7] the hadronic top quark candidate in 25 % of the cases. The observed distribution of the invariant mass (m_{jjj}) of the hadronic top quark candidates in the combined sample shown in Figure 1d demonstrates good agreement of the kinematical information between the data and the signal+background expectation.

4. Dilepton channel

The dilepton $t\bar{t}$ final state is characterized by two isolated leptons with relatively high p_T , missing transverse energy corresponding to the neutrinos from the W leptonic decays, and two b

¹ $m_T(W) = \sqrt{2p_T^l p_T^{\nu}(1 - \cos(\phi^l - \phi^{\nu}))}$ where the E_T^{miss} vector provides the neutrino information.

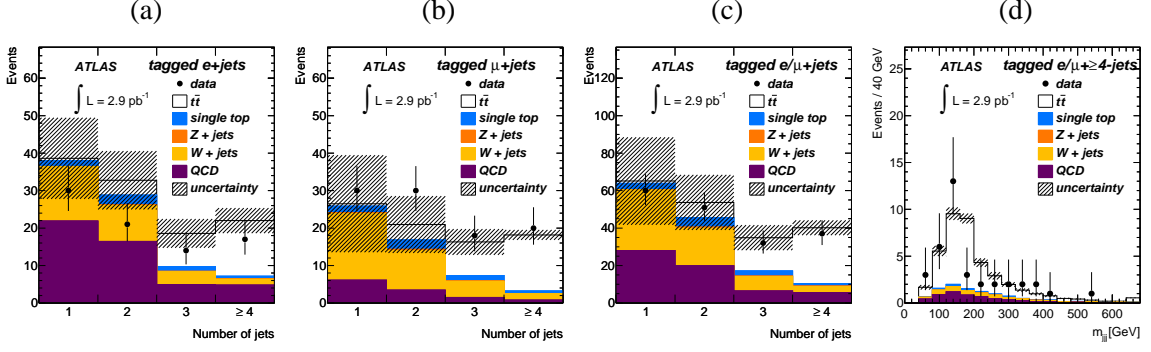


Figure 1: (a) - (c): Jet multiplicity distributions (*i.e.* number of jets with $p_T > 25$ GeV): (a) electron channel, (b) muon channel and (c) electron/muon combined. The data are compared to the sum of all expected contributions.

(d) Distribution of the invariant mass of the 3-jet combination having the highest p_T for the combined sample with ≥ 4 jets. The background uncertainty on the total expectation is represented by the hatched area.

quark jets. Events are required to have exactly two oppositely-charged leptons (ee , $\mu\mu$ or $e\mu$) each satisfying $p_T > 20$ GeV, where at least one must be associated to a leptonic high-level trigger object. Furthermore, at least two jets with $p_T > 20$ GeV and with $|\eta| < 2.5$ are required, but no b -tagging requirements are imposed.

To suppress backgrounds from Z +jets and QCD multi-jet events in the ee channel, the missing transverse energy must satisfy $E_T^{\text{miss}} > 40$ GeV, and the invariant mass of the two leptons must differ by at least 5 GeV from the Z boson mass, *i.e.* $|m_{ee} - m_Z| > 5$ GeV. For the muon channel, the corresponding requirements are $E_T^{\text{miss}} > 30$ GeV and $|m_{\mu\mu} - m_Z| > 10$ GeV. For the $e\mu$ channel, no E_T^{miss} or Z boson mass veto cuts are applied. However, the event H_T , defined as the scalar sum of the transverse energies of the two leptons and all selected jets, must satisfy $H_T > 150$ GeV to suppress backgrounds from Z +jets production.

Finally, to remove events with cosmic-ray muons, events with two identified muons with large, oppositely signed transverse impact parameters ($d_0 > 500 \mu\text{m}$) and consistent with being back-to-back in the $r - \phi$ plane are discarded. The E_T^{miss} , Z boson mass window, and H_T cuts are derived from a grid scan significance optimisation on simulated events which includes systematic uncertainties. The estimated $t\bar{t}$ acceptances including the $t\bar{t}$ branching ratios, given a dilepton event, in each of the dilepton channels are 0.24% (ee), 0.38% ($\mu\mu$) and 0.81% ($e\mu$). The dominant background contributions come from Z +jets (for ee and $\mu\mu$) and from W +jets (for ee and $e\mu$). The latter enters the analysis through jets misreconstructed as leptons. These contributions are estimated using a set of data-driven approaches further detailed in [5]. The smaller sources of background: $Z \rightarrow \tau\tau$, single top and diboson production (WW, WZ and ZZ) are estimated from simulation.

Figure 2 shows the predicted and observed distributions of E_T^{miss} for the ee and $\mu\mu$ channels and of H_T for the $e\mu$ channel. The predicted and observed multiplicities of all jets are compared in Figure 3a-c for each channel individually. Figure 3d shows the same for b -tagged jets for all channels combined. The latter shows that a majority of the selected events have at least one b -tagged jet, consistent with the hypothesis that the excess of events over the estimated background originates from $t\bar{t}$ decay. The number of expected and measured events in the signal region are shown in Table 2. A number of sources of systematic uncertainty are accounted for. The dominant

contributions in the dilepton channel are: luminosity measurement, signal simulation, jet energy reconstruction and background rate normalisation.

	ee	$\mu\mu$	$e\mu$
Observed	2	3	4
Total est. background	0.60 ± 0.27	0.88 ± 0.40	0.97 ± 0.30
$t\bar{t}$	1.19 ± 0.19	1.87 ± 0.26	3.85 ± 0.51

Table 2: Observed event yield, estimated total background and $t\bar{t}$ signal for the ee , $\mu\mu$ and $e\mu$ channels. All systematic uncertainties are included.

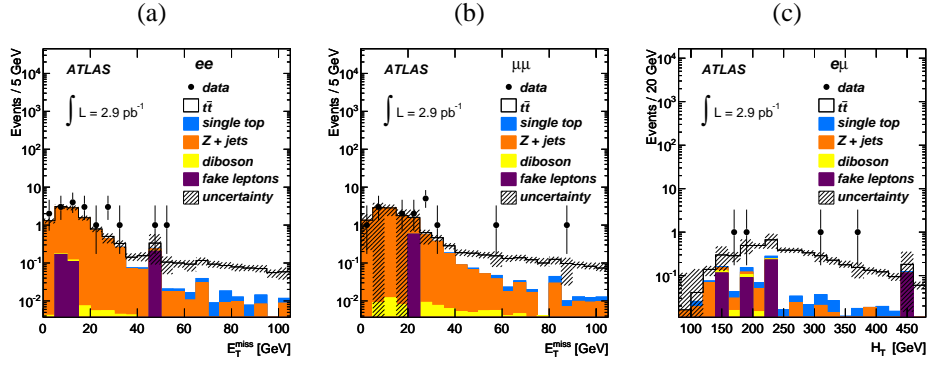


Figure 2: The E_T^{miss} distribution for (a) the ee channel without the $E_T^{\text{miss}} > 40$ GeV requirement, (b) the $\mu\mu$ channel without the $E_T^{\text{miss}} > 30$ GeV requirement, and (c) the distribution of the H_T , defined as the scalar sum of the transverse energies of the two leptons and all selected jets, in the signal region without the $H_T > 150$ GeV requirement.

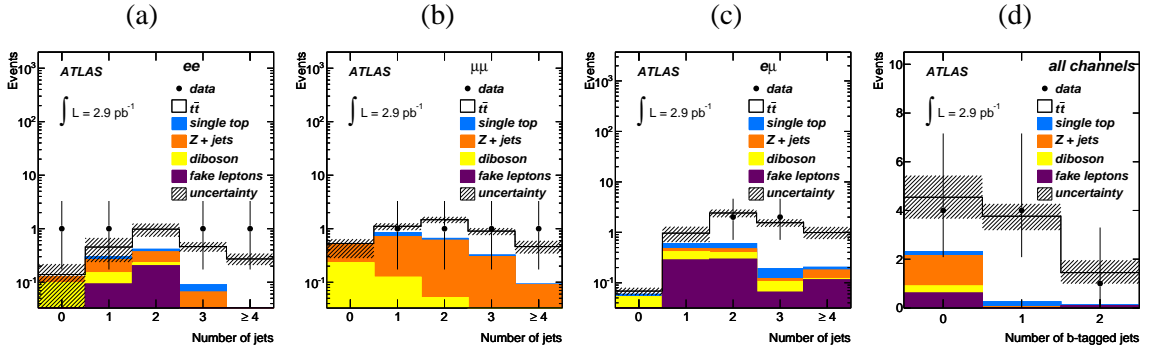


Figure 3: Jet multiplicities for (a) the ee channel, (b) the $\mu\mu$ channel and (c) the $e\mu$ channel. The b -tagged jet multiplicity is shown for (d) the combined dilepton channel with the $N_{jets} \geq 2$ requirement.

5. Cross-section measurement

The cross-section is measured in each decay channel and translated into an inclusive $t\bar{t}$ cross-section using the $W \rightarrow \ell\nu$ and $\tau \rightarrow \ell\nu\nu_\tau$ branching ratios. The combined measurement of the $t\bar{t}$ production cross-section is based on a likelihood fit in which the number of expected events is modeled as

$$N^{exp}(\sigma_{t\bar{t}}, \alpha_j) = L \cdot \varepsilon_{t\bar{t}}(\alpha_j) \cdot \sigma_{t\bar{t}} + \sum_{bkg} L \cdot \varepsilon_{bkg}(\alpha_j) \cdot \sigma_{bkg}(\alpha_j) + N_{DD}(\alpha_j) \quad (5.1)$$

where L is the integrated luminosity, $\varepsilon_{t\bar{t}}$ is the signal acceptance, ε_{bkg} , σ_{bkg} are the efficiency and cross-section for backgrounds as obtained from MC simulation respectively, and N_{DD} is the number of expected events from data-driven estimates. The acceptance and background estimates depend on sources of systematic uncertainty labelled as α_j . Sources of systematic uncertainties are grouped into subsets that are uncorrelated to each other. However each group can have correlated effects on multiple signal and background estimates. Table 3 lists the cross-sections and signal significance for the single-lepton, dilepton and the combined channels with the corresponding statistical and systematic uncertainties extracted from the likelihood fit. By combining all five channels, the background-only hypothesis is excluded at a significance of 4.8σ obtained with the approximate method of [8]. The absence of bias in the fit is validated by pseudo-experiments.

Channel	$\sigma_{t\bar{t}}$ [pb]	Signal significance [σ]
e +jets	$105 \pm 46^{+45}_{-40}$	-
μ +jets	$168 \pm 49^{+46}_{-38}$	-
ee	$193^{+243}_{-152}{}^{+84}_{-48}$	-
$\mu\mu$	$185^{+184}_{-124}{}^{+56}_{-47}$	-
$e\mu$	$129^{+100}_{-72}{}^{+32}_{-18}$	-
Single lepton channels	$142 \pm 34^{+50}_{-31}$	4.0
Dilepton channels	$151^{+78}_{-62}{}^{+37}_{-24}$	2.8
All channels	$145 \pm 31^{+42}_{-27}$	4.8

Table 3: Measured cross-sections in each individual channel and in the combined fit. The uncertainties represent the statistical and combined systematic uncertainty, respectively.

6. Summary

Measurements of the $t\bar{t}$ production cross-section in the single-lepton and dilepton channels using the ATLAS detector are reported. In a combined sample of 2.9 pb^{-1} , 37 $t\bar{t}$ candidate events are observed in the single-lepton topology, as well as 9 candidate events in the dilepton topology, resulting in a measurement of the inclusive $t\bar{t}$ cross-section of

$$\sigma_{t\bar{t}} = 145 \pm 31^{+42}_{-27} \text{ pb.}$$

This is the first ATLAS Collaboration measurement making simultaneous use of reconstructed electrons, muons, jets, b -tagged jets and missing transverse energy, therefore exploiting the full capability of the detector. The cross-sections measured in each of the five sub-channels are consistent with each other and kinematic properties of the selected events are consistent with SM $t\bar{t}$ production. Furthermore, the cross-sections is in good agreement with other measurements and the approximate NNLO top quark cross-section calculation [9]. With the perspective of having a higher statistics data sample, the statistical and systematic uncertainty on the $t\bar{t}$ cross-section will decrease and a precise measurement can challenge the SM prediction based on QCD calculations and constrain the parton distribution functions. Larger samples of $t\bar{t}$ events will also be critical in precision studies of the production, mass and decay properties of top quarks, and be vital in new physics searches in which SM $t\bar{t}$ production is an important background.

References

- [1] S. L. Glashow, Nucl. Phys. **22** (1961) 579; S. Weinberg, Phys. Rev. Lett. **19** (1967) 1264; A. Salam, Elementary Particle Theory, ed. N. Svartholm, (Almqvist and Wiksell, Stockholm, 1968), p. 367.
- [2] S. Moch and P. Uwer, *Theoretical status and prospects for top-quark pair production at hadron colliders*, Phys. Rev. D **78** (2008) 034003;
U. Langenfeld, S. Moch, and P. Uwer, *New results for $t\bar{t}$ production at hadron colliders*, Proc. XVII Int. Workshop on Deep-Inelastic Scattering and Related Topics, dx.doi.org/10.3360/dis.2009.131, hep-ph/0907.2527.
- [3] ATLAS Collaboration, *The ATLAS Experiment at the CERN Large Hadron Collider*, JINST, **3** S08003 (2008).
- [4] ATLAS Collaboration, *Measurement of the $W \rightarrow l\nu$ and $Z/\gamma^* \rightarrow ll$ production cross sections in proton-proton collisions at $\sqrt{s} = 7$ TeV with the ATLAS detector*, JHEP **12** (2010) 060.
- [5] ATLAS collaboration, *Measurement of the top quark-pair production cross section with ATLAS in pp collisions at $\sqrt{s} = 7$ TeV*, accepted by EPJC, hep-ex/1012.1792.
- [6] M. Cacciari, G. P. Salam and G. Soyez, *The anti-kt jet clustering algorithm*, JHEP **0804** (2008) 063.
- [7] ATLAS Collaboration, *Expected Performance of the ATLAS Experiment - Detector, Trigger and Physics*, CERN-OPEN-2008-020, hep-ex:0901.0512, pages 874–881.
- [8] G. Cowan, K. Cranmer, E. Gross and O. Vitelles, *Asymptotic formulae for likelihood-based test of new physics*, submitted to Eur. Phys. J., hep-ex/1007.1727.
- [9] M. Aliev et al., *HATHOR HAdronic Top and Heavy quarks crOss section calculatoR*, hep-ex/1007.1327.